

# Optimizing printing parameters for enhanced mechanical properties of 3D printed PLA octet lattice structures

Oğuz Tunçel<sup>1\*</sup>

<sup>1</sup>Sıirt University, Engineering Faculty, Mechanical Engineering Department, Sıirt, Türkiye

**Orcid:** O. Tunçel (0000-0002-6886-6367)

**Abstract:** 3D printers, known as one of the rapid prototyping methods, are used in research and academic studies as well as industry. This technology makes it easy and fast to produce a preliminary prototype of a design. This study explores the impact of printing parameters on the mechanical properties of 3D-printed octet lattice structures using PLA material. Focused on optimizing layer thickness, print speed, and infill density, the study employed Taguchi methodology. Compressive strength and strength per mass were the key metrics analyzed. The optimized parameters, determined as 0.2 mm layer thickness, 90 mm/s print speed, and 100% infill density, significantly enhanced compressive strength. Infill density emerged as the most influential factor, contributing to 82.75% of the overall variation. A robust predictive model was developed, achieving a 92.06% accuracy in estimating compressive strength per mass values. These findings provide crucial guidelines for manufacturing high-strength, lightweight PLA octet lattice structures, vital in industries like aerospace and automotive. This study advances additive manufacturing, opening avenues for further research in diverse lattice structures and materials.

**Keywords:** Fdm, pla, octet lattice, compression strength, Taguchi, ANOVA

## 1. Introduction

Additive manufacturing (AM) is a versatile industrial manufacturing technique that can produce products in a three-dimensional (3D) structure according to a pre-determined design. It is the process of producing the structure layer by layer. These technologies have a lot of potential for generating efficient structural parts, complicated geometries, and small parts, and they have a lot of potential uses in aerospace, defense, automotive, electronics, tool and die making, energy, and biomedical [1,2]. Fused deposition modeling (FDM) is an important AM method with advantages such as ease of application, low machine and consumable cost, durable part production, and easy replacement of the filament used as consumable [3,4]. FDM is a widely used extrusion technique in which the material is heated, melted, and deposited layer by layer through a nozzle. Normally, the nozzle has horizontal movement capability, while the build platform moves vertically after the completion of each new layer. In certain FDM technologies, the nozzle can move both horizontally and vertically [5,6].

AM enables the fabrication of complicated three-dimensional lattice structures with precise control over the cell, support, and overall structure dimensions and configu-

ration [7]. Lattice structures are designed and manufactured to offer specific properties such as strength, shock absorption, acoustic or visual damping, heat transfer, and thermal insulation, thanks to their lightweight. With additive manufacturing, trusses are produced as lattice structures that provide building units with a predefined design [8]. The cellular unit structure significantly influences the mechanical behavior of truss constructions [9]. Lattice structures can be applied in car bumpers and airplane wings that require energy absorption or wherever a high strength-to-weight ratio is needed [10].

The octet-truss lattice is a highly effective support structure for integrating structure and function because of its inherent porous qualities and remarkable load-bearing capability [11]. The octet-truss truss structure is characterized by a unit cell with 12 equal nodal connections and is typically stress-dominated. These structures are widely used in aerospace, automotive, and medical industries. They can, for example, replace foam materials in lightweight structures such as sandwich panels and offer higher strength-to-density ratios than flexural lattices [12]. The octet truss lattice structure has the potential for an alternative application to foams or honeycomb cellular materials [13].

\* Corresponding author.  
Email: oguz.tuncel@siirt.edu.tr



Literature studies on the compressive strength of FDM-fabricated lattice structures are given below. Rahman et al. [14] achieved optimal results by combining 0.1 mm layer thickness, 205°C printing temperature, 50 mm/s printing speed, and 60°C bed temperature. These parameters yielded the maximum modulus of elasticity and compressive strength, showcasing the significant impact of manufacturing settings on PLA lattice cubic structures in biomedical applications. Dong et al. [15] optimized FDM process parameters for lattice structures using the manufacturable element concept. Layer thickness (0.2 mm, 245°C nozzle, 600 mm/min, 0% fan speed) proved most advantageous for horizontal struts. In contrast, inclined struts were optimized with a layer thickness of 0.1 mm, a nozzle temperature of 255°C, a printing speed of 1200 mm/min, and a fan speed of 50%. Their approach improved mechanical performance, emphasizing the significance of specific parameters for different structural features. Future research will explore the impact of dynamic process parameters on lattice structure quality in FDM fabrication. Dixit and Jain [16] optimized fused filament fabrication process parameters for lattice structures using the Taguchi method with TPU and PLA materials. They determined the optimal combination as 0.1 mm layer thickness, 100% infill density, and 40 mm/s printing speed, maximizing compressive strength. Liu et al. [17] enhanced the FDM technique by introducing a snap-fitting method for fabricating PLA plus BCC lattice structures. Relative densities of 2.1% to 8.3% were achieved, showing significant improvements: 37.6%–65.3% in peak strengths, 11.4%–39.6% in compressive moduli, and 67%–270% in energy absorption per unit volume compared to conventional FDM structures. The method also offered superior surface quality and printing efficiency. Analytical models considering

node volume accurately predicted mechanical properties. This innovative approach can extend to other additive manufacturing technologies like PolyJet. Emir et al. [18] studied the load behaviors of octet-truss lattice structures produced via FDM with varied transition geometries. Compression tests and FEM analyses revealed transition geometry's crucial role in deformation patterns and stress distributions. Structures lacking transitions exhibited plastic deformation at low-stress levels, while transitioned geometries experienced plastic deformation at higher stresses. Deformation areas in straight and inclined transitions were smaller, emphasizing the importance of transition design. Stretch-dominated deformation, impacting lattice strength under load, was consistent across all structures. Zisopol et al. [19] conducted a study on PLA lattice structures through FDM, employing various filling patterns, including octet. The triangle pattern exhibited 98.98% accuracy and 57.70% deformation, reaching a maximum compressive force of 87.32 kN. The octet pattern, along with others, was examined in the research. The optimization of use value to production cost was achieved, emphasizing the economic importance of cubic subdivision and the technical feasibility of octet structures.

Optimizing printing parameters is essential as it directly affects the mechanical properties of the produced part. This study optimized additive manufacturing parameters for superior compressive strength in PLA octet-truss lattice structures. The findings contribute valuable insights for enhancing lattice structures' mechanical properties, emphasizing parameter optimization's importance in additive manufacturing processes. Future research could explore applying similar optimization techniques for different lattice structures and materials, further advancing

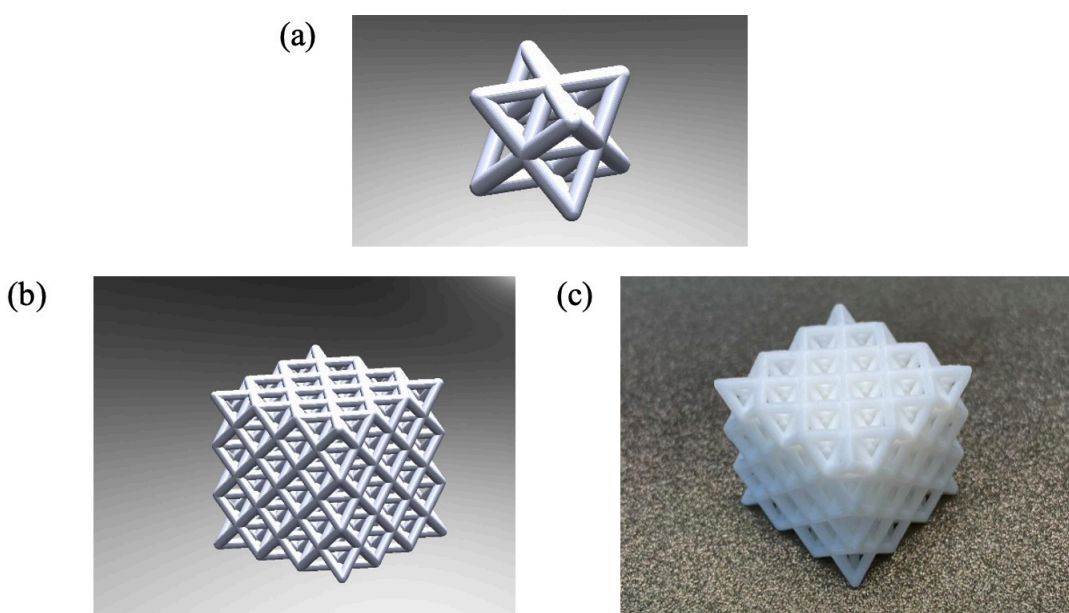


**Figure 1.** The experimental sample having octet-truss lattice structure (a) Octet-truss unit cell,

(b) Solidworks drawing of octet-truss compression specimen consisting of 3x3x3 unit cells, (c) An example of a sample printed with a 3D printer

the field of additive manufacturing.

## 2. Material and Method

This study used poly(lactic acid) PLA filament as the experimental material. PLA is an organic biopolymer and thermoplastic produced from corn starch and sugar cane [20]. Therefore, it is not harmful to human health. The filament used is Creality brand, white, and 1.75 mm thick. It has 1.24 g/cm<sup>3</sup> density, 51 MPa tensile, 86 MPa compression, and 10.5 J impact strength. For compression tests, specimens consisting of cubic octet-truss lattice structures with dimensions of 30 mm x 30 mm x 30 mm are shown in Figure 1 [21,22]. The unit lattice structure has dimensions of 10 mm x 10 mm x 10 mm and a circular cross-section with a strut diameter of 1.75 mm (Figure 1a) [18]. The drawing of the printed specimen consisting of 3x3x3 unit cells for a total of 27 unit cells using the Solidworks 2020 program is shown in Figure 1b. An example of a sample printed with a 3D printer is shown in Figure 1c. As shown in Figure 1b in the Solidworks 2020 drawing program, the sample CAD file prepared in STL format was transferred to the Cura 5.4.0 program for parameter entries. Thanks to this program, the drawing is converted into G codes that the 3D printer can recognize. There is also the flexibility to change the parameters that affect the print quality as much as the printer's capacity allows.

Minitab 20.3 program was used to create the experimental design. The experimental design was performed utilizing the Taguchi methodology. The parameter changes were related to the defined output value of strength per unit mass. The experiments were designed with three different parameters and three levels. With the full factorial design, 3<sup>3</sup> total 27 experiments should be performed, while Taguchi L9 design was selected, and 9 experiments were used to reach the optimum output. The printing parameters and levels are given in Table 1, and the Taguchi L9 experimental design is given in Table 2. Printing processes were carried out using the Creality brand Ender 3S-1 Pro 3D printer. The masses of the test samples were measured after 3D printing using an analytical scale. The scale used is Shimadzu brand and can measure with an accuracy of 1 in 10000 grams. Taguchi analyses were performed using the larger is better approach using the equation in Equation 1 [23,24]. By means of tables created using signal-to-noise ratios (S/N ratio), the optimum output level for each parameter was selected, and Taguchi results were predicted. The effects of the parameters on the output were determined by analysis of variance (ANOVA). Thanks to ANOVA, we can see the percentage contribution of each parameter to the output. To support the ANOVA analysis, a Pareto Chart is also used to show whether the contribution of the parameters to output is significant or insignificant [25]. In addition, the relationship between output and input parameters was equated by creating a linear regression equation. Such equations allow us to obtain results for intermediate values of the parameters. Finally, the accuracy of the data obtained

from the equation was compared with the consistency of the experimental results.

**Table 1.** Print parameters and levels

Parameters	Unit	Level 1	Level 2	Level 3	Output
Layer thickness	(mm)	0.10	0.20	0.30	Strength per mass (MPa/g)
Print speed	(mm/s)	30	60	90	
Infill density	(%)	60	80	100	

$$\frac{S}{N_{max}} = -10 \log \left( \frac{1}{n} \sum_{i=1}^n \frac{1}{y_i^2} \right) \quad (1)$$

**Table 2.** Three parameters three level Taguchi L9 orthogonal experiment design

No	Layer thickness (mm)	Print speed (mm/s)	Infill density (%)
1	0.1	30	60
2	0.1	60	80
3	0.1	90	100
4	0.2	30	80
5	0.2	60	100
6	0.2	90	60
7	0.3	30	100
8	0.3	60	60
9	0.3	90	80

Three samples were 3D printed for each experimental group and subjected to compression tests using the UTEST brand tensile-compression device. These tests were carried out at room temperature, with a constant feed rate of 1 mm/min [26]. The experimentally obtained results were averaged from the three specimens in each group, and standard deviations were considered to ensure accuracy. Figure 2 is an image of a specimen after compression testing.

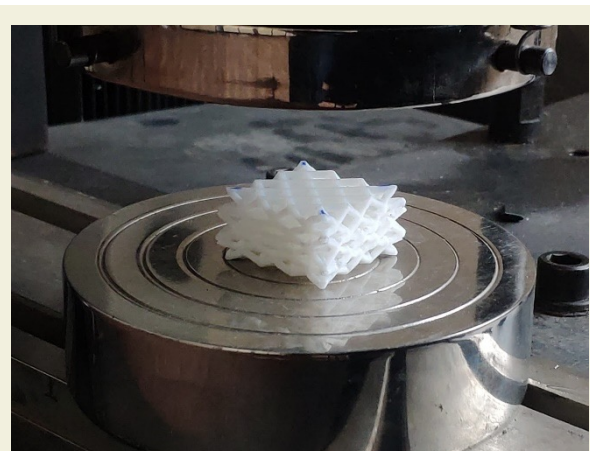


**Figure 2.** The image of a specimen subjected to compression test

### 3. Results and Discussion

The strength and strength per mass values obtained from the compression test are given in Table 3. According to Table 3, the highest compressive strength was obtained as 7.93 MPa in sample 3. The sample with the lowest compressive strength, sample 1, has a compressive strength of 4.62 MPa. The obtained strength values in this study were divided based on sample masses to assess the correlation between parameter variations and compressive strength more precisely [27–29]. The lowest strength per mass value was 0.472 MPa/g for sample 1, while the highest strength per mass value was 0.637 MPa/g for sample 3. The strength per mass value obtained in sample code 3 is 35% higher than that of sample code 1. When Table 3 is analyzed, it is seen that the infill density parameter is effective on the output. When considering the S/N ratios calculated as a result of Taguchi analysis, it is seen that the lowest value is in the sample coded 1 (-6.521), and the highest value is in the sample coded 3 (-3.917) (Table 3).

**Table 3.** Compression values with the calculated S/N ratios

No	Strength (MPa)	Mass (g)	Strength per mass (MPa/g)	Standard deviation	S/N ratio
1	4.62	9.79	0.472	0.011	-6.521
2	6.49	11.24	0.577	0.011	-4.776
3	7.93	12.45	0.637	0.028	-3.917
4	6.18	11.22	0.551	0.017	-5.177
5	7.92	12.49	0.634	0.028	-3.958
6	5.01	9.73	0.515	0.013	-5.764
7	7.07	12.50	0.565	0.008	-4.959
8	4.66	9.78	0.476	0.011	-6.448
9	6.20	11.22	0.552	0.020	-5.161

The S/N ratios response table generated from Taguchi analysis shows the S/N ratios for each level value of the parameters (Table 4). In the table, S/N values with high S/N ratios in each parameter maximize the output [30]. In this case, the 2nd, 3rd, and 3rd levels of layer thickness, print speed and, infill density parameters are effective on

strength per mass, respectively. According to Table 4, in order to reach the optimum output, manufacturing should be done with 0.2 mm layer thickness, 90 mm/s, and 100% infill density parameters. The higher the delta value, the higher the order of influence of the parameters on the output. When Table 4 is analyzed, the order of the effect of the parameters on the output is filling density, printing speed, and layer thickness.

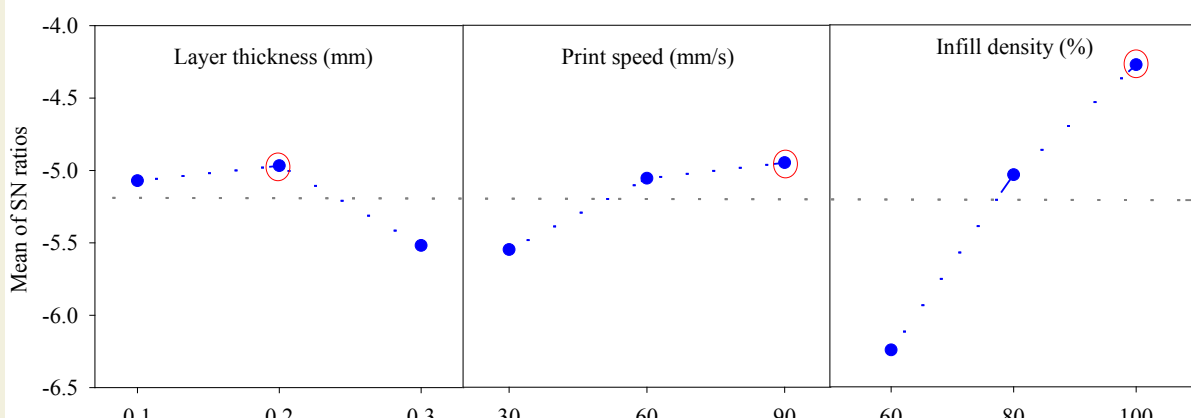
**Table 4.** Response table for the S/N ratios of the strength per mass values (S/N: Larger is better)

Level	Layer thickness (mm)	Print speed (mm/s)	Infill density (%)
1	-5.072	-5.552	-6.244
2	-4.966*	-5.061	-5.038
3	-5.523	-4.947*	-4.278*
Delta	0.556	0.605	1.966
Rank	3	2	1

\*Optimum level

The main effects plot for S/N ratios is given in Figure 3. Here, parameter levels above the mean line indicate that they are sufficient for the desired output levels [31]. 0.1–0.2 mm for layer thickness, 60–90 mm/s for print speed, and 80–100% for infill density are the parameter levels that will provide above-average strength per mass results. The points enclosed in red circles in Figure 3 also indicate the optimum parameter levels.

Table 5 displays the outcomes of the analysis of variance (ANOVA) for the parameter variations within the specified ranges investigated in the study. At the same time, Figure 4 illustrates the percentage contributions of these parameters to strength per mass. Analyses were performed at a 95% confidence level. When the P-value in Table 5 is less than 0.05, the parameters affect on the output [32]. In this case, the table shows that all three parameters affect on strength per mass. The highest contribution to strength per mass is infill density, which is 82.75%. The parameter with the second highest contribu-

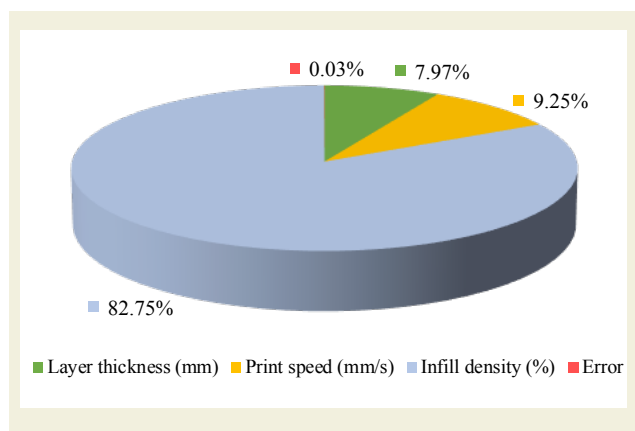


**Figure 3.** S/N ratio graph of parameters for strength per mass values

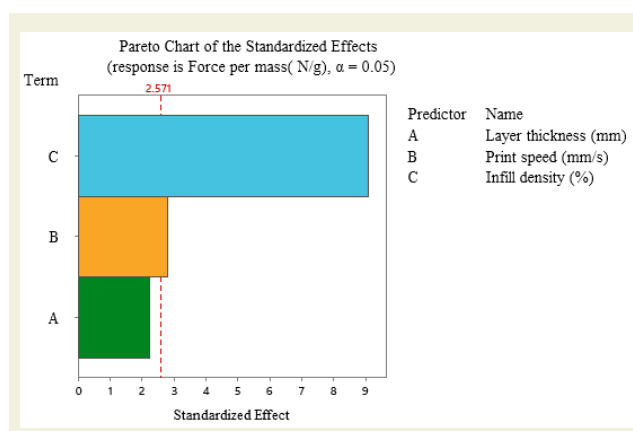
**Table 5.** Analysis of variance (ANOVA) results for strength per mass values

Source	(DoF)	Sq SS	Contribution (%)	F-Value	P-Value
Layer thickness (mm)	2	0.002215	7.97	235.98	0.0042
Print speed (mm/s)	2	0.002616	9.25	273.79	0.0036
Infill density (%)	2	0.023395	82.75	2448.30	0.0004
Error	2	0.000010	0.03	---	---
Total	8	0.028276	100	---	---

tion is the print speed, with 9.25%, while layer thickness has the lowest contribution, with 7.97%. The error rate in the study is very low (0.03%). The  $R^2$  value obtained according to the model is 99.97%.

**Figure 4.** Effect of parameters on strength per mass as a percentage

The Pareto chart in Figure 5 shows the effect levels of the parameters. Parameters with a standardized effect value above the reference line (2.571) are shown as effective. In this case, infill density and print speed parameters are more effective. The standardized effect value of infill density is remarkable. The values obtained in the parato chart graph are consistent with the ANOVA table in Table 5.

**Figure 5.** Pareto chart showing the effects of the parameters

According to Table 4 and Figure 3, the highest strength per mass output parameters were 0.2 mm layer thickness, 90 mm/s print speed, and 100% infill density. When predicted in the Minitab program with these parameter levels, the result was -3.818 for the S/N ratio and 0.640 MPa/g for predicted strength per mass (Table 6). According to the experimental result, the value per mass was 0.643. The error rate between the predicted and experimentally obtained values is as low as 0.47%. According to the results in Table 3, the highest strength per mass value was 0.637 MPa/g in sample 3. The value of 0.643 MPa/g obtained in the sample created with the optimum parameters is 0.94% higher than that of 0.637 MPa/g obtained in the initial design.

**Table 6.** Predicted optimum value and validation of experiment result

Optimum Level: 233	Predicted Value (MPa/g)	Experimental Result (MPa/g)
	0.640	0.643
Prediction Error (%)	0.47	

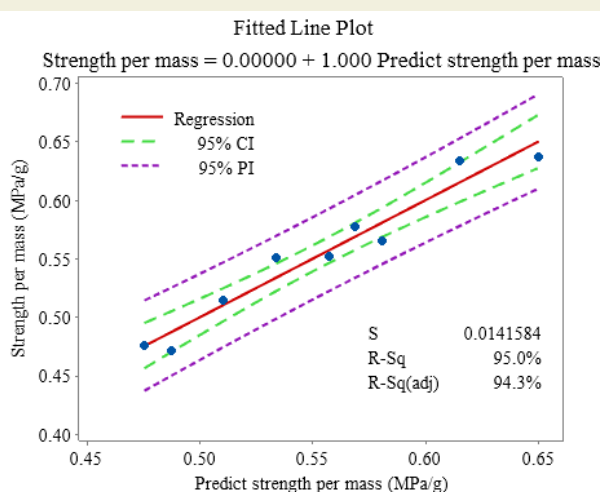
A linear regression equation was created to predict the change in strength per mass with the evolution of parameter change (Table 7). This equation also provides results for parameter levels or combinations not in the design. The  $R^2$  value of the equation is also as high as 92.06%.

Figure 6 compares the predicted strength per mass values with the individual strength per mass results. A comparison of the predictions and results in Figure 6 shows that an efficient analysis is obtained from results close to the regression line. Most points fell within the 95% confidence interval. The  $R^2$  ( $R$ -sq) value of the linear regression model obtained for these comparisons, such as those shown in Figure 6, was calculated at 95%.

Figure 7 shows the experimental strength per mass results and the predicted strength per mass values according to the equation in Table 7. As seen in Figure 7, the strongly predicted data matched well with the obtained results. This showed that the equation with an  $R^2$  value of 92.06% made high predictions.

**Table 7.** Linear regression equation for prediction of strength per mass values (MPa/g)

Strength per mass (MPa/g) = 0.2965-0.1550*Layer thickness +0.000644*Print speed+0.003108*Infill density
R-sq= 92.06%



**Figure 6.** Predicted compression values compared with experimental results for compression per mass values

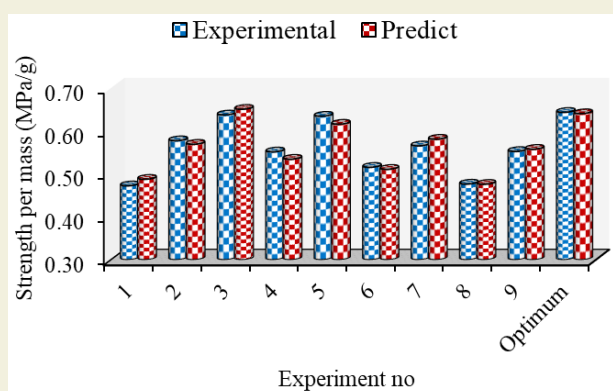


**Figure 7.** Predicted versus experimental results for strength per mass values

## 4. Conclusions

This study investigated the effect of printing parameters on the mechanical properties of 3D-printed octet lattice structures using PLA material. The Taguchi methodology was employed to optimize the printing parameters:

layer thickness, print speed, and infill density. The compressive strength and strength per mass values were used as the leading indicators to evaluate the performance of the lattice structures. The results of the study revealed the following key findings:

- Through Taguchi analysis, the optimized printing parameters for superior compressive strength were determined to be 0.2 mm layer thickness, 90 mm/s print speed, and 100% infill density.
- The study highlighted the significant influence of infill density on the strength per mass of PLA octet lattice structures, contributing to 82.75% of the overall variation.
- A high level of accuracy was achieved in predicting the compressive strength per mass values using the optimized parameters, with an error rate of only 0.47%. Also, the developed linear regression equation demonstrated a strong predictive capability with an R-squared value of 92.06%.
- The optimized parameters and the predictive model can serve as valuable guidelines for manufacturing PLA octet lattice structures with enhanced mechanical properties. These structures find applications in various industries, including aerospace, automotive, and medical fields, where lightweight components with high strength-to-density ratios are essential.
- Future research could explore applying similar optimization techniques for different lattice structures and materials, expanding the scope of additive manufacturing in producing efficient and lightweight components for diverse applications.

In conclusion, this study contributes valuable insights into optimizing 3D printing parameters for enhancing the mechanical properties of lattice structures, paving the way for advancements in additive manufacturing technologies and their industrial applications.

## References

- [1] Vijayakumar, M.D., Palaniyappan, S., Veeman, D., Tamiselvan, M., (2023). Process Optimization of Hexagonally Structured Polyethylene Terephthalate Glycol and Carbon Fiber Composite with Added Shell Walls. *Journal of Materials Engineering and Performance*. 32(14): 6434–47. doi: 10.1007/s11665-022-07572-z.
- [2] Di Angelo, L., Di Stefano, P., Dolatnezhadsomarin, A., Guardiani, E., Khorram, E., (2020). A reliable build orientation optimization method in additive manufacturing: the application to FDM technology. *International Journal of Advanced Manufacturing Technology*. 108(1–2): 263–76. doi: 10.1007/s00170-020-05359-x.
- [3] Stephen Oluwashola Akande., (2015). Dimensional Accuracy and Surface Finish Optimization of Fused Deposition Modelling Parts using Desirability Function Analysis. *International Journal of Engineering Research And. V4(04)*. doi: 10.17577/ijertv4is040393.
- [4] Kamer, M.S., Temiz, Ş., Yaykaşlı, H., Kaya, A., Akay, O., (2022). Effect of Printing Speed on Fdm 3D-Printed Pla Samples Produced Using Different Two Printers. *International Journal of 3D Printing Technologies and Digital Industry*. 6(3): 438–48. doi: 10.46519/ij3dptdi.1088805.
- [5] Tagliaferri, V., Trovalusci, F., Guarino, S., Venettacci, S., (2019). Environmental and economic analysis of FDM, SLS and MJF additive manufacturing technologies. *Materials*. 12(24). doi: 10.3390/ma1224161.
- [6] Do an, O., Kamer, M.S., (2023). Experimental investigation of the creep behavior of test specimens manufactured with fused filament fabrication using different manufacturing parameters. *Journal of the Faculty of Engineering and Architecture of Gazi University*. 38(3): 1839–48. doi: 10.17341/gazimmfd.1122973.
- [7] Silva, R.G., Estay, C.S., Pavez, G.M., Viñuela, J.Z., Torres, M.J.,

- (2021). Influence of geometric and manufacturing parameters on the compressive behavior of 3d printed polymer lattice structures. *Materials*. 14(6). doi: 10.3390/ma14061462.
- [8] Ali, H.M.A., Abdi, M., Sun, Y., (2022). Insight into the mechanical properties of 3D printed strut-based lattice structures. *Progress in Additive Manufacturing*. (0123456789). doi: 10.1007/s40964-022-00365-9.
- [9] Qin, D., Sang, L., Zhang, Z., Lai, S., Zhao, Y., (2022). Compression Performance and Deformation Behavior of 3D-Printed PLA-Based Lattice Structures. *Polymers*. 14(5). doi: 10.3390/polym14051062.
- [10] Zare Shiadehi, J., Zolfaghari, A., (2023). Design parameters of a Kagome lattice structure constructed by fused deposition modeling: a response surface methodology study. *Iranian Polymer Journal (English Edition)*. 32(9): 1089–100. doi: 10.1007/s13726-023-01196-3.
- [11] He, W., Luo, W., Zhang, J., Wang, Z., (2023). Investigation on the fracture behavior of octet-truss lattice based on the experiments and numerical simulations. *Theoretical and Applied Fracture Mechanics*. 125(April): 103918. doi: 10.1016/j.tafmec.2023.103918.
- [12] Li, Y., Gu, H., Pavier, M., Coules, H., (2020). Compressive behaviours of octet-truss lattices. *Proceedings of the Institution of Mechanical Engineers, Part C: Journal of Mechanical Engineering Science*. 234(16): 3257–69. doi: 10.1177/0954406220913586.
- [13] Song, J., Zhou, W., Wang, Y., Fan, R., Wang, Y., Chen, J., et al., (2019). Octet-truss cellular materials for improved mechanical properties and specific energy absorption. *Materials and Design*. 173: 107773. doi: 10.1016/j.matdes.2019.107773.
- [14] Rahman, M.M., Sultana, J., Rayhan, S. Bin., Ahmed, A., (2023). Optimization of FDM manufacturing parameters for the compressive behavior of cubic lattice cores: an experimental approach by Taguchi method. *International Journal of Advanced Manufacturing Technology*: 1329–43. doi: 10.1007/s00170-023-12342-9.
- [15] Dong, G., Wijaya, G., Tang, Y., Zhao, Y.F., (2018). Optimizing process parameters of fused deposition modeling by Taguchi method for the fabrication of lattice structures. *Additive Manufacturing*. 19: 62–72. doi: 10.1016/j.addma.2017.11.004.
- [16] Dixit, N., Jain, P.K., (2022). Effect of Fused Filament Fabrication Process Parameters on Compressive Strength of Thermoplastic Polyurethane and Polylactic Acid Lattice Structures. *Journal of Materials Engineering and Performance*. 31(7): 5973–82. doi: 10.1007/s11665-022-06664-0.
- [17] Liu, W., Song, H., Wang, Z., Wang, J., Huang, C., (2019). Improving mechanical performance of fused deposition modeling lattice structures by a snap-fitting method. *Materials and Design*. 181: 108065. doi: 10.1016/j.matdes.2019.108065.
- [18] Emir, E., Bahçe, E., Uysal, A., (2021). Effect of Octet-Truss Lattice Transition Geometries on Mechanical Properties. *Journal of Materials Engineering and Performance*. 30(12): 9370–6. doi: 10.1007/s11665-021-06096-2.
- [19] Zisopol, D.G., Tănase, M., Portoacă, A.I., (2023). Innovative Strategies for Technical-Economical Optimization of FDM Production. *Polymers*. 15(18): 3787. doi: 10.3390/polym15183787.
- [20] Jayasekara, T., Wickrama Surendra, Y., Rathnayake, M., (2022). Polylactic Acid Pellets Production from Corn and Sugarcane Molasses: Process Simulation for Scaled-Up Processing and Comparative Life Cycle Analysis. *Journal of Polymers and the Environment*. 30(11): 4590–604. doi: 10.1007/s10924-022-02535-w.
- [21] Mora, S., Pugno, N.M., Misseroni, D., (2022). 3D printed architected lattice structures by material jetting. *Materials Today*. 59(October): 107–32. doi: 10.1016/j.mattod.2022.05.008.
- [22] Raz, K., Chval, Z., Sedlacek, F., (2020). Compressive strength prediction of quad-diametral lattice structures. *Key Engineering Materials*. 847 KEM: 69–74. doi: 10.4028/www.scientific.net/KEM.847.69.
- [23] Almetwally, A.A., (2020). Multi-objective Optimization of Woven Fabric Parameters Using Taguchi-Grey Relational Analysis. *Journal of Natural Fibers*. 17(10): 1468–78. doi: 10.1080/15440478.2019.1579156.
- [24] Jagatheesan, K., Babu, K., (2023). Taguchi optimization of minimum quantity lubrication turning of AISI-4320 steel using biochar nanofluid. *Biomass Conversion and Biorefinery*. 13(2): 927–34. doi: 10.1007/s13399-020-01111-3.
- [25] Abdulredha, M.M., Hussain, S.A., Abdullah, L.C., (2020). Optimization of the demulsification of water in oil emulsion via non-ionic surfactant by the response surface methods. *Journal of Petroleum Science and Engineering*. 184(July 2019): 106463. doi: 10.1016/j.petrol.2019.106463.
- [26] Bouteldja, A., Louar, M.A., Hemmouche, L., Gilson, L., Miranda-Vicario, A., Rabet, L., (2023). Experimental investigation of the quasi-static and dynamic compressive behavior of polymer-based 3D-printed lattice structures. *International Journal of Impact Engineering*. 180(May): 104640. doi: 10.1016/j.ijimpeng.2023.104640.
- [27] Almesmari, A., Sheikh-Ahmad, J., Jarrar, F., Bojanampati, S., (2023). Optimizing the specific mechanical properties of lattice structures fabricated by material extrusion additive manufacturing. *Journal of Materials Research and Technology*. 22: 1821–38. doi: 10.1016/j.jmrt.2022.12.024.
- [28] Galeta, T., Raos, P., Stojšić, J., Pakši, I., (2016). Influence of structure on mechanical properties of 3D printed objects. *Procedia Engineering*. 149(June): 100–4. doi: 10.1016/j.proeng.2016.06.644.
- [29] Sood, M., Wu, C., (2023). Influence of 3D printed structures on energy absorption 17(4): 390–405.
- [30] Hikmat, M., Rostam, S., Ahmed, Y.M., (2021). Investigation of tensile property-based Taguchi method of PLA parts fabricated by FDM 3D printing technology. *Results in Engineering*. 11: 100264. doi: 10.1016/j.rineng.2021.100264.
- [31] Ahmad, M.N., Ishak, M.R., Mohammad Taha, M., Mustapha, F., Leman, Z., Anak Lukista, D.D., et al., (2022). Application of Taguchi Method to Optimize the Parameter of Fused Deposition Modeling (FDM) Using Oil Palm Fiber Reinforced Thermoplastic Composites. *Polymers*. 14(11). doi: 10.3390/polym14112140.
- [32] Wankhede, V., Jagetiya, D., Joshi, A., Chaudhari, R., (2019). Experimental investigation of FDM process parameters using Taguchi analysis. *Materials Today: Proceedings*. 27: 2117–20. doi: 10.1016/j.matpr.2019.09.078.